Construction and Building Materials 104 (2016) 247–262

Contents lists available at ScienceDirect

Construction and Building Materials

journal homepage: www.elsevier.com/locate/conbuildmat

Static and dynamic properties of concrete with different types and shapes of fibrous reinforcement

Aiman Hasan Hamood Al-Masoodi, Ahmed Kawan, Mudiono Kasmuri, R. Hamid *, M.N.N. Khan

Department of Civil and Structural Engineering, Faculty of Engineering and Built Environment, Universiti Kebangsaan Malaysia, 43600 UKM Bangi, Selangor, Malaysia

HIGHLIGHTS

- Concrete are reinforced with different types and shapes of fibres.
- Split Hopkinson Pressure Bar (SHPB) is used to study the dynamic properties of the FRC.
- W-shape steel FRC shows the superior static and dynamic behaviours.
- PP fibres slightly reduce the static, but improve the dynamic properties of concrete.
- 5% coir fibre had enhanced concrete dynamic stress, at par with W-shape steel fibre.

ARTICLE INFO

Article history:
Received 22 May 2015
Received in revised form 3 November 2015
Accepted 6 December 2015

Keywords:
Fibre-reinforced concrete (FRC)
Steel
Polypropylene (PP)
Coir
Static properties
Dynamic properties

ABSTRACT

This research determines the static compressive, split tensile and flexural strengths as well as dynamic stress, strain and toughness of fibre-reinforced concrete (FRC) at strain rates of 30–50 s^{-1} (single impact pressures of 2 and 3 MPa). Three fibre types (steel, polypropylene (PP) and coir (CF)) with different shapes, sizes, lengths and contents are considered. The newly modified W shape steel fibre has the greatest influence on concrete static and dynamic properties. PP fibre slightly reduces the concrete mechanical properties, but improves the dynamic properties 15% more compared to plain concrete (PC). The compressive strength of 5% CF concrete is slightly improved, but the flexural and split tensile strengths are improved by 11% and 35%, respectively, compared to PC. There are significant improvements in dynamic stress, strain and toughness due to addition of 5% CF in concrete. CF stands at par with steel fibre in enhancing both the static and dynamic properties of FRC.

1. Introduction

Concrete structures may be exposed to loading within short time periods such as earthquakes, impacts and explosions during their service lives. Concrete responds differently to dynamic loading compared to static loading. Plain (unreinforced) concrete (PC) has high compressive strength but poor tensile strength (at approximately one tenth of its compressive strength) and low resistance to tensile cracking due its brittle characteristic. For this reason, the strain capacity of PC is inadequate for absorbing energy and resisting impact loads. Concrete structures must be designed to resist dynamic loads by improving the material's capacity to absorb shock energy. The brittle characteristics of concrete members can be ameliorated by adding fibres. When added to the concrete mix as reinforcements, fibres have the potential to increase the bond of the Portland cement paste and the concrete matrix and improve the mechanical properties. The primary role of fibre in a concrete mix is to reduce and control the speed of tensile cracking propagation by keeping the crack widths to a minimum. By adding fibres into a concrete mix, unstable tensile crack propagation is transformed to a slow, controlled crack growth. Therefore, the inclusion of fibres in concrete reduces the acceleration of shear and flexural crack propagation. Furthermore, the addition of fibre enhances the ductility of the concrete and thereby improves its energy absorption capacity. Additionally, fibre can provide better resistance to high strain rate loadings compared to PC. The tensile and compressive stresses of fibre reinforced concrete (FRC) are enhanced more than PC when loaded at high strain rates.

Fibre reinforcements such as horsehair and straw in mortar and sun-dried adobe bricks have been used in building materials for centuries [1]. Currently, many fibre types such as steel, synthetic, glass and natural fibres are specifically designed and manufactured for structural development purposes. Natural reinforcing materials

* Corresponding author.

http://dx.doi.org/10.1016/j.conbuildmat.2015.12.037
0950-0618/

can be obtained at low cost and with low levels of energy consumption by using local manpower and technology. The utilisation of natural fibre as a form of concrete reinforcement is of particular interest in less-developed regions where conventional construction materials are not readily available or expensive.

Vajje and Murthy [2] used different types of natural organic fibres, including jute, sisal, hemp, banana and pineapple, in order to study the properties of concrete. They concluded that the inclusion of natural organic fibres may have improved some concrete properties and reduced others, as each fibre exhibited its own unique properties. However, Sivaraja et al. [3] found that the addition of natural fibres (coir and sugarcane) enhanced the compressive, split tensile and flexural performance of concrete. Ramakrishna and Sundararajan [4] prepared slabs reinforced with coconut, sisal, jute and hibiscus cannabinus (kenaf) fibres in order to test impact resistance. They reported that a coconut fibre content of 2% and a fibre length of 40 mm demonstrated the best performance by absorbing 253.5 J of impact energy. They also mentioned that at ultimate failure, all fibres (except coconut fibres) exhibited fibre fracture, whereas coconut fibre showed fibre pull-out. Agopyan et al. [5] used both coir and sisal fibres as replacements for asbestos in roofing tiles and performed a three-point bend test. Their test results showed that the maximum load endured by the coir tiles was much higher than the sisal tiles. Therefore, coconut fibre is considered the most useful and inexpensive type of natural fibre for use in concrete composites. Significant research on coir fibre-reinforced concrete (CFRC) already exists, and it is generally accepted that the optimum content of coir fibre varies as the source of coir fibre changes. The optimum coir fibre content, by mass of cement, obtained by previous studies ranges between 0.5% and 5%.

The static properties of CFRC have been studied by numerous researchers. It has been determined that the flexural strength of CFRC is much greater than that of PC [6–8]. In contrast, Ali et al. [9] found that the modulus of rupture (MOR) for PC beams is typically higher than those of CFRC beams. According to their study, the MOR of CFRC with 5% fibre content and 5-cm fibres slightly increased to 4% when compared to PC. In addition, the split tensile strength of CFRC significantly increased [8–10]. The compressive strength of CFRC has been determined in numerous existing studies. Some researchers have reported that the compressive strength of CFRC has increased from 11% to 24% [8,9]. However, some researchers reported on the negative influence of coir on the compressive strength of CFRC [10,11].

The dynamic properties of CFRC have also been studied by various researchers. Coir fibres were used by Cook et al. [12] as reinforcement in low-cost roofs. They measured the impact resistance of coir fibre-reinforced cement roofs by dropping a 50-mm diameter 0.53 kg steel ball onto the centre of the sample. They found that the impact index of the coir fibre-reinforced cement roofs increased with increase in fibre volume and length. Similarly, a drop-weight impact test was conducted by Ali et al. [9] in order to evaluate the damping ratio and fundamental frequency of coir fibre-reinforced beams. According to their test results, a higher coir fibre content led to increased damping; however, the static and dynamic elastic modulus decreased. They concluded that the optimum coir fibre length and content were 5 cm and 5% by mass of cement, respectively. More recently, Wang and Chouw [13] carried out a study to investigate the behaviour of CFRC under impact loading. The coir fibre used in their study was 5 cm in length, and the coir fibre content was 0.4% by total weight of the concrete mix. A comparison between the PC and CFRC impact behaviours was reported in their study. Based on their results, the energy absorption capacity of CFRC was much higher than that of PC. It was also observed that the impact behaviour of PC featured brittle failure, whereas the tested CFRC specimens exhibited ductile failure with small cracks.

Significant research has also been carried out regarding fibre-reinforced concrete (FRC) using steel, polyvinyl alcohol (PVA) and polypropylene (PP). In recent decades, the application of steel fibre-reinforced concrete (SFRC) has consistently increased due to its significantly improved properties. It is currently applied in airport and highway pavement, earthquake and impact-resistant structures, tunnels, bridges and hydraulic structures [14]. A significant literature related to the FRC is discussed comprehensively in the "State-of-the-Art Report on Fiber Reinforced Concrete" published by ACI committee 544. According to this article the behaviour of FRC depends on number of factors [15]. Erdogmus, 2015 [16] categorized those factors as base matrix characteristics, fibre characteristics and composite mixture characteristics.

Tan et al. [17] reported compressive and flexural strength increases of up to 30% through the addition of steel fibre. According to Nagarkar et al. [18], the compressive, split tensile and flexural strengths of steel fibrous concrete increased by up to 13–40% when steel fibres are added at different aspect ratios and volume fractions. In addition, the inclusion of steel or PVA fibres in concrete significantly increases other properties such as stress–strain resistance, impact resistance, resistance to flexural fatigue and ductility [7,19–22]. It was observed that the addition of steel fibres increased the increment of compressive and split tensile strength of concrete by up to 30%, whereas the addition of PP fibres only increased these tensile strength increments by 4% compared with PC fibres [23]. Aliabdo et al. [19] also found that specimens reinforced with steel fibres showed considerably better behaviour when compared to specimens reinforced with PP fibres. The static and dynamic properties of concrete reinforced with coir, steel, PVA and PP, as obtained from existing literature, are presented in Tables 1 and 2.

Some researchers have added mineral admixtures such as fly ash (FA), silica fume (SF) and metakaoline to the FRC in order to enhance the mechanical properties of FRC. The optimal portion of silica fume (SF) is approximately 5% for improving the mechanical properties [24,25], and the concrete strengths increased significantly with the fibre content and SF addition [26,27].

A review of the above studies shows that only a few studies investigated the dynamic properties of CFRC. It should also be noted that a Split Hopkinson Pressure Bar (SHPB) apparatus was not used to investigate the dynamic properties of CFRC. Therefore, this study uses a SHPB to investigate the dynamic properties of CFRC with different contents of coir fibre. However, the crucial factor of FRC is impact resistance, and numerous experiments have been previously conducted using various fibre shapes and material types with different equipment [28]. The impact load is generated by either sticker bar impinging in an SPHB test [17,20,21,29–31] or dropping weights [1,32–34]. In this study, three different shapes of steel fibre types i.e., Hook-Ended Steel Fibre (HKSF), Proposed Steel Fibre I (γ-shape) (PSFI), Proposed Steel Fibre II (W-shape) (PSFII), and two types of PP fibre (PPI & PPII) were also considered to study the dynamic and static properties of FRC (reinforced with steel and PP). Namaan introduced steel fibres having a tri-dimensional configuration for use as reinforcement for Portland cement concrete matrices in his patent article **US 3852930 A** [35]. Namaan and co-workers had conducted vast researches in order to investigate the various properties of FRC using Hook-Ended Steel Fibre and also other shapes [36–38]. Namaan, 2003 also proposed newly developed twisted fibres named as torex fibres with their several advantages in cement matrices [39]. In present study, the two types steel fibres are modified based on gap of the previous studies. Studies and results on other fibre types have not been as extensive or as conclusive as those on steel fibres.

Table 1
Previous researches on static mechanical properties of concrete reinforced with various fibres.

Type of fibre	Length (cm)	Fibre content (%)	Aspect ratio	Compressive strength (MPa)	Flexural strength (N/mm^2)	Split tensile strength (MPa)	Absorption capability	Ductility	Note	Researchers
Coir	1.25, 2.5, 3.8	2[a], 3[a], 4[a]	–	–	3% fibre with length 2.5 cm are recommended to obtain 22 N/mm^2 strength	–	–	–	0.15 N/mm^2 casting pressure	Paramasivam et al. [6]
Coir	2, 4	1.5[b]	–	–	Increase 12%	–	Increase 16.80%	Increase 17.40%	–	Li et al. [7]
Steel	6	0.5[a], 1[a]	80	Increase 19%	Increase 1.94 times	Increase 62%	–	–	Higher water/(cement + fibre) ratio shows good results	Nili & Afroughsabet [8]
Coir & sugarcane		1.5[a]	60	Increase 11.3%	Significant enhancement	Increase 9.14%	–	–	Increment of strength does not depend greatly on curing period	Sivaraja et al. [3]
Coir	2.5, 5, 7.5	1[c], 2[c], 3[c], 5[c]	–	Increase 24%	No improvement	Increase or decrease up to 11%	–	–	Recommend 5% fibre with length 5 cm	Ali et al. [9]
Jute, Sisal, Hemp	0.6, 1	0.5[c], 1[c], 1.5[c]		Slight increase	–	–	–	–	Young's modulus increase slightly	Vajje & Murthy [2]
Coir	–	3[b]	–	–	–	–	–	–	40% shear strength improvement	Gampathi [11]
Coir	–	0.5[a]	125	Adversely affected	–	Significant increase	Significant increase	–	–	Yalley and Kwan [10]
Steel & PVA	2.4, 1.2, 0.6, 1.2, 3.0, 2.7, 3.0	0.5[a], 1[a], 2[a]	340, 400, 40, 60, 60, 50, 45, 75	Increase 2–5 MPa	Increase 15%	–	–	Significant increase	2% fibre content shows the best results in all tests	Suraneni et al. [20]

a – by volume; b – by weight; c – by mass of cement; – data not available.

Table 2
Previous researches on dynamic properties of concrete reinforced with various fibres.

Type of fibre	Length (cm)	Fibre content (%)	Aspect ratio	Stress–strain curve	Flexural fatigue failure	Modulus of elasticity (dynamic)	Impact resistance	Toughness	Note	Researchers
Coir	2.5, 3.75, 6.35	2.5[a], 5[a], 7.5[a], 10[a], 15[a]	–	–	–	–	Significant increase	–	–	Cook et al. [12]
Steel	6	0.5[a], 1[a]	80	–	–	–	Remarkable improvement	–	–	Nili & Afroughsabet [8]
Steel	1.3	1.5[a], 3[a]	–	Remarkable improvement	–	–	Remarkable improvement	Remarkable improvement	Toughness energy is proportional to the fibre content	Wang et al. [29]
Coir	2.5, 5, 7.5	1[c], 2[c], 3[c], 5[c]	–	–	–	Remarkable improvement	–	Remarkable improvement	Higher damping values while lower frequency	Ali et al. [9]
Steel	30–34, 50–52, 50–55	1[a],2[a]	38–43, 56–58, 56–61	–	–	–	Increase 21–59%	–	16–22% reduction in penetration	Aliabdo et al. [17]
Steel	3,4	1[a], 1.5[a]	80–60	Significant increase	–	–	–	–	Stress–strain curves under different strain rates are derived (50 s^{-1} to 200 s^{-1})	Hao & Hao [18]
PVA	0.6	0.1[a]	–	–	Increase resistance	For 150 cycle, 71% in plain concrete and 80 % in fibred concrete	–	–	Flexural fatigue test using a wheel load was performed with a stress level in the range of 0.5–0.9	Jang et al. [19]
Steel	3.5	0.5[a], 1[a], 1.5[a]	64	Significant increase	–	–	Remarkable improvement	Significant increase	Dynamic impact was performed at strain rate of 30–60 s^{-1}	Tan et al. [15]

a – by volume; c – by mass of cement; – data not available

2. Research significance

A review of the existing literature indicates that significant research has been conducted regarding the static properties of CFRC. However, there is limited research on the dynamic properties of CFRC. Therefore, this research describes the mechanical properties (compressive, flexural, and split tensile strengths) of CFRC as well as the dynamic stress–strain response of CFRC based on the impact resistance investigated by using a SHPB under a strain rate of 30–50 s^{-1}. Similarly, several studies have already been published regarding the behaviour of FRC (reinforced with steel, PVA or PP) under static and dynamic loads. None of these studies systematically examined the influences of different shapes and material types of FRC with SF that are subjected to dynamic load. Therefore, the purpose of this research is to study the fibre effects based on the performance of their shapes and material types on the dynamic stress, strain and energy absorption capacity of FRC with SF under impact loading at different levels. Five fibre types with different shapes and material properties were investigated in this research. The properties of FRC with SF were studied using tests for compressive, split tensile and flexural strengths for mechanical properties and impact tests for dynamic properties.

3. Materials and methods

3.1. Materials

3.1.1. Cement

Ordinary Portland cement Type I (OPC) was used as the cementitious material in this experimental work for all concrete mixes. It conforms to the ASTM C150 [40] standard. It has a specific gravity of 3.12 and a Blaine specific surface area of 380 m^2/g. The initial and final setting times were 74 min and 385 min, respectively.

3.1.2. Silica fume (SF)

Silica fume (SF) is a by-product in the production of silicon and ferrosilicon alloys. It has a greater surface area than cement approximately 2090 cm^2/g due to its small particle size. Therefore, a concrete mix containing SF usually requires more water. Thus, an SF dosage of 5% by weight of cement is added to the FRC mixes.

3.1.3. Fine aggregate

Dry and clean natural river sand was used as fine aggregate and passed through a 4.75-mm sieve. The fine aggregate has a specific gravity of 2.59, a fineness modulus of 2.98 and water absorption of 0.93%. The loose and compacted bulk density values of the fine aggregate are 1600 and 1688 kg/m^3, respectively.

3.1.4. Coarse aggregate

Crushed granite aggregate available from local sources was used as coarse aggregate. The maximum size of the coarse aggregate is no more than 10 mm and has a specific gravity of 2.65, a fineness modulus of 5.95 and water absorption of 0.46%. The loose and compacted bulk density values of the coarse aggregates are 1437 and 1526 kg/m^3, respectively.

3.1.5. Superplasticiser (SP)

Polycarboxylate-based superplasticiser (SP) (Viscocrete-2044) was used in this research as an aqueous modified solution. It has a specific gravity of 1.08. It was used to achieve the desired workability of the PP fibre-reinforced concrete mixtures. The dosage of SP is 0.5% by weight of cement.

3.1.6. Fibres

3.1.6.1. Steel and PP fibres. The major variables used in the study are three different shapes of steel fibre types (Hook Ended Steel Fibre (HKSF-35 mm), Proposed Steel Fibre I (γ-shape) (PSFI-35 mm) and Proposed Steel Fibre II (W-shape) (PSFII-35 mm)) and two types of Polypropylene Fibre (PPI and PPII), as shown in Fig. 1. A constant 1% volume fraction dosage of all fibre types is used. The properties of the different fibre types are listed in Table 3. PSFI is manually fashioned from Hook-Ended Steel Fibre (HKSF-60 mm). Each HKSF-60 mm fibre is bent at the middle of the fibre into a spiral shape by keeping both ends hooked as shown in Fig. 1. PSFII (W-shaped) is also fashioned manually from the same HKSF-60 mm fibre. Three nails are driven on a plywood to create the γ and W-shape and steel fibres are shaped through this nails figuration to assure the consistency of these fibres. Bundles of HKSF-60 mm fibre were manually bent to a type of wave shape (W) with a 35-mm length. This modification develops the bond between the steel fibre and the concrete matrix due to its detoured shape and provides a strong anchorage mechanism. Moreover, both ends exhibit hooked characteristics that will provide greater impact resistance.

3.1.6.2. Coir fibre. The coir fibre used in this study is locally available. For the static test specimens, the fibres were cut to lengths of 3–5 cm with scissors. For the dynamic test specimens, the fibres were cut to lengths of 1–2 cm because of the need for smaller specimens. The average diameter of the fibre used was 0.48 mm. Therefore, the aspect ratio of the coir fibre used in the static tests was 62.5–104.2, while the aspect ratio of fibre used in dynamic test was 20.83–41.66. The fibres were washed to remove dust and dried by spinning in a drying machine. They were then kept in the open air to assure total dryness. The properties of the coir fibres are shown in Table 3.

3.2. Mixture proportions and preparation

3.2.1. Mixture proportions and preparation of FRC

The mix design is calculated in accordance with the British Department of Environment method (DOE Method of Concrete Mix Design). According to the mix design, the targeted compressive strength is 30 MPa and the water–cement ratio is 0.54, with a water content of 230 kg/m^3 and a cement content of approximately 426 kg/m^3. The recommended slump should be maintained between 30 and 60 mm with this water–cement ratio. SP was added to 0.5% by weight of cement for the PP fibre mixes to increase the workability without segregation and bleeding. The concrete mixture proportions of each cubic meter of concrete are shown in Table 4.

All specimen moulds were lubricated with oil in order to facilitate the removal of samples from the moulds. Fresh PC1 and each type of FRC (HKSF, PSFI, PSFII, PPI and PPII) containing fibres of 1% of volume fraction were prepared. First, coarse and fine aggregate were mixed together for 2 min in dry conditions. Second, the cement and fibres were mixed with 10% of the water for 2 min. Third, 80% of the water was added and mixed for another 2 min. Fourth, the remaining 10% of the water and the SF dosage of 5% by weight of cement were added and mixed for approximately 3 min to prepare the FRC, while 0.5% of SP (by weight of cement) was added into the PP-reinforced concrete mixes to maintain their workability. Finally, the freshly mixed FRC was cast into the moulds in three layers. After pouring each layer, the moulds were vibrated in order to remove any trapped air. Each specimen was allowed to stand for 24 h in the laboratory before demoulding. Specimens were marked and immersed in water at approximately 21–25 °C until the age tests at 3, 7 and 28 days.

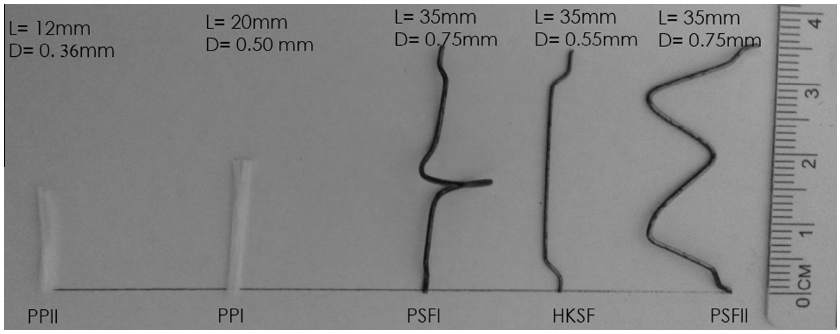

Fig. 1. Different types and shapes of fibres.

Table 3
Properties of different types of fibre.

Fibres	Length (mm)	Equivalent diameter (μm)	Tensile strength (MPa)	Density (kg/m^3)	Elastic modulus (GPa)	Ignition temperature (°C)	Melting temperature (°C)
HKSF	35	55	1300	7850	200	–	–
SFPI	35	75	1300	7850	200	–	–
SFPII	35	75	1300	7850	200	–	–
PPI	23	50	350	910	4.2	600	165
PPII	12	36	325	900	4	600	165
CF	100–500	480	–	2057	–	–	–

Data not available

Table 4
Mixture design proportions.

Mix. No	Fibre content (%)	w/c	Water (kg/m^3)	Cement (kg/m^3)	SF (kg/m^3)	Fine aggregate (kg/m^3)	Coarse aggregate (kg/m^3)	SP (kg/m^3)
PC1	0	0.54	230	405	21	908	806	0
HKSF	1[a]	0.54	230	405	21	908	806	0
SFPI	1[a]	0.54	230	405	21	908	806	0
SFPII	1[a]	0.54	230	405	21	908	806	0
PPI	1[a]	0.54	230	405	21	908	806	2.13
PPII	1[a]	0.54	230	405	21	908	806	2.13
PC2	0	0.45	230	377	0	917	847	0
CFRC1	1[c]	0.46	230	377	0	917	847	0
CFRC3	3[c]	0.50	230	377	0	917	847	0
CFRC5	5[c]	0.53	230	377	0	917	847	0

a – by volume; c – by mass of cement.

3.2.2. Mixture proportions and preparation of CFRC

The mix design was calculated according to the British Department of Environment method (DOE Method of Concrete Mix Design). Four different mixes were used to prepare the test specimens PC2, CFRC1, CFRC3 and CFRC5. The detailed mix designs are shown in Table 4.

Two types of mixing procedures were adopted for the preparation of the CFRC. Both mechanical and manual mixing procedures were adopted considering some constructions for low cost housing in rural areas are still practising manual mixing. For the specimens used in the compressive and flexural strength tests, a horizontal pan mixer with a capacity of 80 kg was used, whereas manual mixing was adopted for the specimens used in the impact and split tensile strength tests.

3.2.2.1. Mixing procedure using horizontal pan mixer.

- **PC2**

The mix components were placed into the pan mixer and mixed for approximately 2 min. Three quarters of the water was added according to a water–cement ratio of 0.45, and the pan was allowed to rotate for another 2 min. Finally, the remaining water was added to the mix and mixed for another 3 min. The concrete mix was then poured into the moulds in three layers, where each layer was vibrated on a vibrating table for 10 s. Twenty four hours later, specimens were removed from the moulds and immersed in water for 3, 7 and 28 days.

- **CFRC**

In order to cast the CFRC, initial aggregates were placed into the pan mixer in approximately three equal layers. A portion of the coir fibre was then uniformly distributed on the aggregate. After completing the placement of the total quantities of aggregate and coir fibre, the mixer was rotated for 2 min. The addition of water during the casting of the CFRC was similar to the mixing procedure of PC2. However, an extra amount of water was required in order to obtain a workable CFRC mix because of the water absorption ability of the dry coir fibres.

3.2.2.2. Manual mixing procedure.

- **PC2**

In the manual mixing procedure, all concrete components were placed in the mixing tray and mixed thoroughly by hand. The concrete mix was then poured into cylindrical moulds in three layers. After pouring each layer, the mould was vibrated for approximately 10 s. Twenty four hours later, the specimens were removed from the moulds and immersed in water for 3, 7 and 28 days.

- **CFRC**

The manual mixing procedures for CFRC were nearly identical to the manual mixing procedures for PC2. An extra amount of water was added to obtain a workable concrete mix.

Different mixing procedures were adopted for FRC and CRFC due to the extra amount of water required in order to obtain a workable CFRC mix because of the high water absorption of the dry CF. On the other hand, FRC mix (steel and PP) with addition of small amount of superplasticizer (0.5% by weight of cement) already gave workable mix with fixed water content according to the mix design. In addition, SF dosage of 5% by weight of cement is added to the FRC mixes only.

3.3. TESTING

3.3.1. Compressive strength

Concrete cubic specimens of 100 mm^3 were cast in steel moulds for the compressive strength tests for each mix of FRC and CFRC. The average compressive strength values of the four specimens were recorded at 3, 7 and 28 days. The entire test was carried out according to BS EN 12390-3 [41] by using a compressive testing machine with a loading capacity of 5000 kN.

3.3.2. Split tensile strength

The splitting tensile strengths of both FRC and CFRC were determined according to ASTM 496/C496 M-2004 [42] and BS 1881-117:1983 [43], respectively, using concrete cylindrical specimens of 100 mm $\times$ 200 mm. The splitting tensile tests of the FRC specimens were performed at 3, 7 and 28 days of curing age, whereas the CFRC specimens were tested at 28 days. In order to perform the splitting tensile test, the compressive testing machine was used with a different loading apparatus.

3.3.3. Flexural strength

The flexural tests of FRC and CFRC were carried out according to BS 1881-118 [44] using prisms specimens of 100 $\times$ 100 $\times$ 500 mm. The flexural strength of the FRC specimens was tested at 28 days, whereas the CFRC specimens were tested at 3, 7 and 28 days.

3.3.4. Impact test

A SHPB system was used in this study to test the dynamic behaviour under impact loading. An SHPB system is shown in Fig. 2 (a) & (b) and consists of a launch tube, a striker bar, pulse shaper (brass), an incident bar, a transmission bar, two strain gauges and a signal conditioner connected to an oscilloscope (OMB-DAQ-3000) and computer. The measurement system uses a velocity and dynamic strain indicator. The Young's modulus of the projectile, incident and transmission bar is 210 GPa, with a wave velocity of 5190 m/s.

The cylindrical specimen of 50 mm $\times$ Ø50 mm which was the size same as the bars was placed in between the incident bar and the transmission bar. The specimen surface in contact with the incident and transmission bar was polished to attained high precision of levelness and smoothness for test under uniaxial compression using a sticker bar, as shown in Fig. 2(c). The striker bar hits the thin brass pulse shaper mounted on the incident bar. The brass pulse shaper functions as signal shaper to obtain better stress pulse that propagated into the incident bar and to the concrete specimen. When the striker bar with velocity, V_0 before impact at time, $t < 0$, hits the incident bar, an incident stress pulse is generated at $t > 0$. This pulse propagates to the interface between the bar and the specimen through one-dimensional wave propagation theory along the incident bar. At this point, a portion of the pulse is reflected back along the incident bar as a tensile pulse, and the remaining portion is transmitted from the specimen to the transmission bar as a compressive wave signal pulse and recorded by a strain gauge. If the striker/incident bars interface velocity after impact is V and the velocity of the striker bar during impact is V_s, it can be shown that:

$$V = V_0 - V_s \tag{2.1}$$

The velocity of the particles of the incident bar at the interface of the striker/incident bar is: $V = V_1$, so that Eq. (2.1) becomes:

$$V_1 = V_0 - V_s \tag{2.2}$$

In this manner, the incident bar measures the incident and reflected pulses and the transmission bar measures the transmitted pulse [29]. The strain signal is recorded using a high-speed 10-bit digital oscilloscope that connects to the computer. A schematic diagram of the SHPB system is shown in Fig. 3a).

The most optimum bar diameter (50 mm) were chosen to count for alignment of bars and friction between bars and their supports and also to reduce severe dispersion of waves due to bigger diameters of bars. The specimen's dimension had to be reduced to get higher strain rate loading on the specimen. The specimen dimension of 50 mm diameter and 50 mm length was found to be the most optimum, also to take into account of effect of axial and radial inertia, thus the designed geometry and size of the specimen. Actual steel fibre length of 35 mm is the mostly commercially available and that length is applied in its application.

To minimize experimental errors, the recorded strain gauges signals were improved by keeping good contact between bars and specimen by levelling the specimen surface with hand grinder and sand paper, reducing the friction between bars and supports, keep good contact between bar surface and strain gauges, keeping bars well coaxial using laser alignment to precision up to 0.01 mm for the specimen to satisfy the stress equilibrium condition (Figs. 3b and 3c). Fig. 3c shows the incident wave if there is fiction and the incident wave without friction.

The signal dispersion correction was also applied. Fig. 3d shows the flow chart of the analysis of the dispersion of wave in the bars. Computer program was written in MatLab®.

Once all three pulses are recorded, the stress, strain rate and strain histories of the specimen in uniaxial compression can be computed, respectively, using Eqs. (2.3)–(2.5) [17,29,30].

$$\sigma(t) = \frac{AE}{2A_s}[\varepsilon_i(t) + \varepsilon_r(t) + \varepsilon_t(t)], \tag{2.3}$$

$$\dot{\varepsilon}(t) = \frac{c_0}{L_s}[\varepsilon_i(t) - \varepsilon_r(t) - \varepsilon_t(t)], \tag{2.4}$$

$$\varepsilon(t) = \frac{c_0}{L_s}\int_0^t [\varepsilon_i(t) - \varepsilon_r(t) - \varepsilon_t(t)]dt. \tag{2.5}$$

$\varepsilon_i(t)$, $\varepsilon_r(t)$ and $\varepsilon_t(t)$ are the surface-strain time histories induced by the incident, reflected and transmitted waves, respectively; c_0, A and E are the wave velocity, cross-sectional area and Young's modulus of the pressure bars , respectively; L_s and A_s are the length and cross-sectional area of the specimen. The expression for the strain rate in Eq. (2.4) is integrated with respect to time to provide the strain in Eq. (2.5).

3.4. Samples

A total number of 280 specimens (168 FRC + 112 CFRC) were tested in this study.

Fig. 2. View of the SHPB system: (a) SHPB equipment; (b) signal conditioner with oscilloscope connected to a computer and (c) concrete specimen between incident bar and transmission bar.

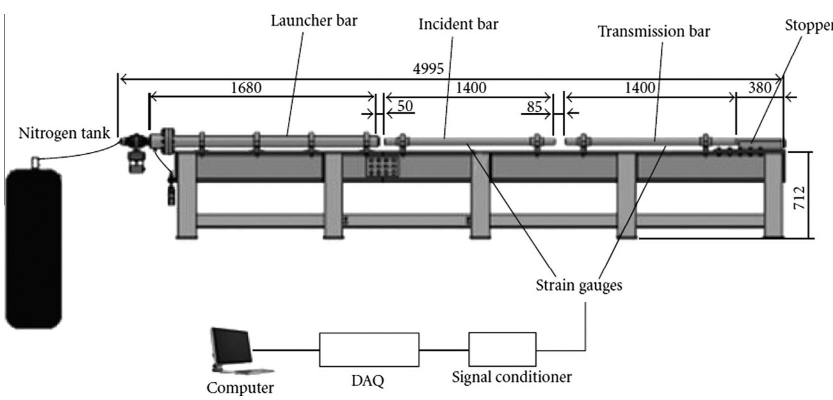

Fig. 3a. Schematic diagram of split Hopkinson pressure bar system (all measured distance in mm) [15].

4. Results and discussion

4.1. Static properties

4.1.1. Compressive strength

The compressive strengths of PC (PC1 & PC2) and the five types of FRC specimens containing steel fibre and CFRC (CFRC1, CFRC3 and CFRC5) at 3, 7 and 28 days are shown in Fig. 4. In the FRC, each type has a different shape or material but the same volume. It can be seen that there is an increase in compressive strength for the three different steel fibre-reinforced concrete specimens, varying from 18% to 28%, 23% to 31% and 15% to 27% at 3, 7 and 28 days, respectively, when compared with PC1.

Fig. 4 also shows that the PSFII reinforced concrete shows the maximum increment in compressive strength at all mixes and ages when compared to PC1. This is because of the modified bundle-shaped fibres that reduce the risk of balling and disperse the fibres uniformly during the concrete mixing process. In addition, it demonstrated a better anchorage bond, which can provide extra resistance to cracking because of its modified 'W' shape, thus increasing the compressive strength. The total percentage increments in compressive strength of the PSFII reinforced concrete were 28.2%, 30.87% and 27.48% compared to PC1 at 3, 7 and 28 days, respectively. Xu et al. [31] reported 23.2%, 28.17% and 20.78% increments in compressive strength at 3, 7 and 28 days when using a Hook-Ended Steel Fibre (HKSF). However, Eren and Celik [26], Song and Hwang [45] and Tan et al. [17] found increments in compressive strength to be no more than 15% from the addition of HESF to concrete. The PSFI reinforced concrete showed a lower compressive strength compared to the PSFII and SFHK reinforced concrete at all ages. This may be due to the modification of the HKSF 60-mm bundles into single-shaped fibres; as a result, they may have lost some water-soluble glue. In addition, the results show that both the PPI and PPII fibre-reinforced concretes had respective increments in compressive strength of 9.2–7.22% and 7.25–3.43% between 3 and 7 days when compared to PC1. However, at 28 days, the compressive strengths reduced, respectively, by approximately 3.4% and 8.9%. The compressive strength was slightly increased with a 1% volume fraction of synthetic fibre according to a study by Xu et al. [33]. Topcu and Canbaz [23] found that compressive strength increases with less than 0.5% volume fraction of PP fibre.

In Fig. 4, the compressive strength of PC2 at 7 days is equal to approximately 77.9% of its compressive strength at 28 days,

Fig. 3b. Laser alignment of the bars.

whereas the compressive strengths of CFRC1, CFRC3 and CFRC5 at 7 days are equal to approximately 79.2%, 74.7% and 63.3% of their compressive strengths at 28 days, respectively. Therefore, it can be concluded that a higher content of coir fibre results in less compressive strength gain at early curing. Fig. 4 indicates that the compressive strength was slightly improved with the addition of 3% and 5% coir fibre content. The obtained maximum compressive strength improvement was 7% when 3% coir fibre was added. In contrast, Ali et al. [9] noted that the compressive strength of CFRC decreased as the coir fibre content increased. In their research, the maximum increase in compressive strength was 23% for a 1% addition of coir fibre in concrete. However, current research shows no significant improvement in compressive strength due to the addition of 1% coir fibre in concrete.

Therefore, based on the obtained results, CRFC is not suitable for higher compressive strength purposes, whereas FRC made from PSFII with SF can provide significant compressive strength. In addition, PP-fibre concrete has a negative or slight influence on compressive strength.

4.1.2. Split tensile strength

Fig. 5 shows the Split Tensile strength of PC and the various fibre-reinforced concrete specimens at different ages. The tensile strength of the PSFII reinforced concrete is greater among all types of fibre-reinforced concrete, with increments of 28.1%, 36.9% and 49.9% when compared to PC1 at 3, 7 and 28 days, respectively. However, the HKSF reinforced concrete shows respective increases in tensile strength of approximately 26.6%, 32.1% and 41.2% at these stages. Many studies have reported that the addition of steel fibres (hook ended) in concrete can improve split tensile strength by up to 20% [23,25,45,46]. However, the PSFI reinforced concrete shows only small increments of approximately 1.1%, 7.1% and 1.1% at 3, 7 and 28 days, respectively, due to the balling risk. In addition, the PSFI fibres cling to each other because of the individual spiral geometry, which reduces the bond between the concrete and the fibres. In general, the splitting tensile strength of FRC depends on the shape, material and formation of individual fibres or bundles of reinforced fibre.

In Fig. 5, it is obvious that the tensile strength of PP (PPI & PPII) fibre-reinforced concrete is lower than PC1 at all ages. Hughes and Fattuhi [47] also found lower tensile strength for PP-reinforced concrete than PC. The addition of PP fibre causes a decrement in split tensile strength compared to PC1. This is because of the 1% addition of PP fibre, which is greater than the 0.5% of volume fraction limit; this can cause poor workability and lead to the entrapment of large amounts of air in the mixtures. Topcu and Canbaz [23] found that concrete reinforced with PP at less than 0.5% of volume fraction has an increment of split tensile strength of approximately 30–4% with the addition of 10–20% fly ash. It can be shown that the tensile strength of FRC mixtures exhibits similar behaviour to their compressive strength. In other words, the increment of the splitting tensile strength of FRC is directly proportional to the increment of its compressive strength [48].

As shown in Fig. 5, the split tensile strengths of CFRC1 and CFRC5 significantly improved compared to PC2, at approximately 19.5% and 34.7%, respectively. However, CFRC3 did not show any significant improvement in split tensile strength. The result obtained for CFRC3 totally contrasts with the results obtained for CFRC1 and CFRC5, which strongly indicate that an error occurred during the preparation, handling and/or testing of the specimens. Therefore, the result obtained for CFRC3 is ignored. Ali et al. [9] found a 16.2% maximum increment in split tensile strength for a 2% addition of coir fibre in concrete; however, they reported an 8% reduction in split tensile strength for a 5% addition of coir fibre in concrete, which is much lower than these results.

4.1.3. Flexural strength

Fig. 6 represents the flexural performance of PC and the different FRC specimens. The PSFII reinforced concrete mix shows the highest increment in flexural strength, at approximately 58.7% of PC1. However, PSFI shows only a 2.6% increment in flexural strength when compared to PC1. This may due to the interruption of mixing in the preparation of beams using PSFI. However, the HKSF reinforced concrete shows significant flexural strength at approximately 47% of PC1. Mohammadi et al. [46] and Tan et al. [17] also reported that the flexural strength of FRC can be enhanced by up to 35% with a 1% volume fraction of steel fibre.

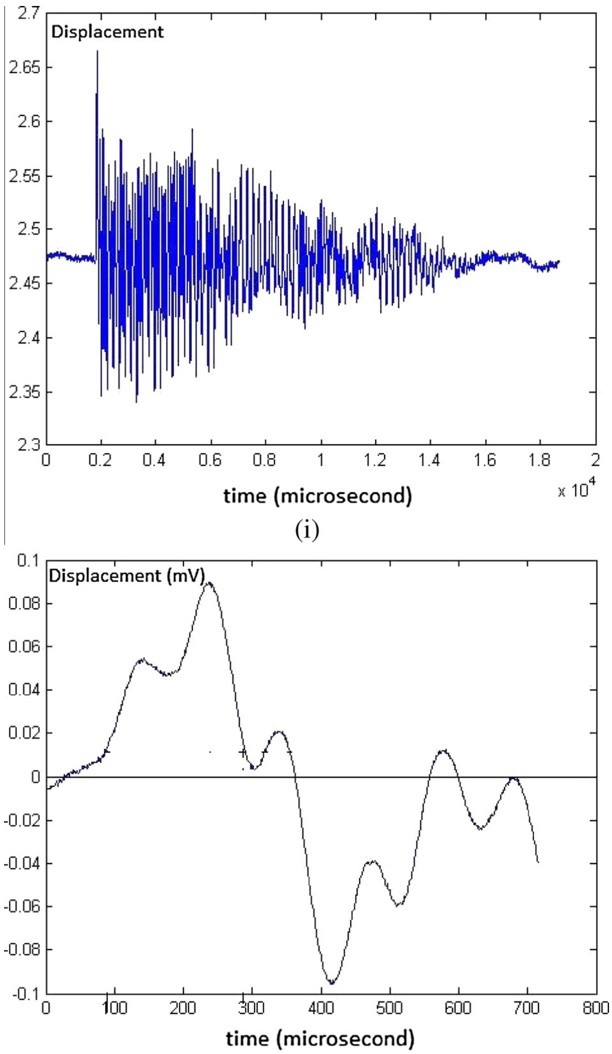

Fig. 3c. (i) Incident wave if there is fiction and (ii) incident wave without friction.

Conversely, the PPI and PPII reinforced concretes show a 12.1% and 16.3% decrease in flexural strength compared to PC1, respectively. It should be noted that the density of PP-reinforced concrete is lower than PC1; thus, the addition of higher amounts of PP fibre will reduce the concrete strength.

In Fig. 6, the flexural strength of PC2 at 7 days is equal to 88.7% of its flexural strength at 28 days. However, the flexural strengths of CFRC1, CFRC3 and CFRC5 at 7 days are equal to 87.6%, 86.3% and 75.9% of their flexural strengths at 28 days, respectively. Therefore, it can be concluded that a higher content of coir fibre results in lower flexural strength gain at the early stages of curing. Fig. 6 also shows that the flexural strength of CFRC is significantly improved as the coir fibre content increases. An 11% maximum improvement of flexural strength is obtained with a 5% coir fibre content. Ali et al. [9] found a slight improvement in the flexural strength of concrete with the addition of 3% and 5% coir fibre. However, they reported a 21% reduction in the flexural strength of concrete with the addition of 1% coir fibre.

4.2. Dynamic properties

The dynamic properties of the PC (PC1 & PC2), FRC (HKSF, PSFI, PSFII, PPI and PPII) with SF and CFRC (CFRC1, CFRC3 & CFRC5) specimens were investigated in this study with a single impact test. Thus, the pressure of the impact velocity was adjusted at 2 MPa and 3 MPa to determine the strain rate of the specimens.

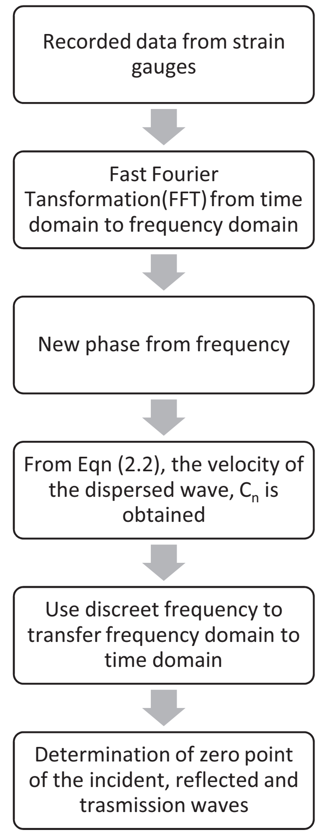

Fig. 3d. Flow chart of the analysis of the dispersion of wave in the bars.

4.2.1. Ultimate stress

Figs. 7a and 8a show the stress–strain curves for concrete specimens with and without reinforced fibre at 2 and 3 MPa of pressure, as obtained by using an SHPB system with strain rates of 30–50 s^{-1}. The strain rate for each specimen is unique, as mentioned in Figs. 7a and 8a, because the deformation rate of each specimen is affected by the material properties under the same impact load. As shown in Figs. 7b and 8b, the ultimate stress of PSFII is greater than the other steel and polypropylene fibre types due to its superior anchorage bond and mechanical deformation capability. This may due to its shape, which leads to a more significant rate of sensitivity to strength. Compared to PC1, the increments of the PSFII reinforced specimens are approximately 86.2% and 70% for impact pressures of 2 and 3 MPa, respectively. However, the PSFI reinforced specimen has an increase in ultimate stress of approximately 74.9% and 56% at these pressures. This is due to the spiral geometry, which improves the bond, and the proper manual mixing of the fibres, which decreases the risk of balling and clinging fibres. However, the HKSF reinforced specimen shows a lower increment compared to the PSFII and PSFI reinforced specimens, which are 44.2% and 34.9%, respectively. This is due to the presence of only anchorage parts in the HKSF fibre ends. There is an increase in the ultimate stress of the PP-reinforced specimens compared to PC1; the ultimate stress of the PPII reinforced specimen is greater than the PPI reinforced specimen at two different pressures. Therefore, it can be concluded that the ultimate stress of different FRC specimens are significantly affected by the shape

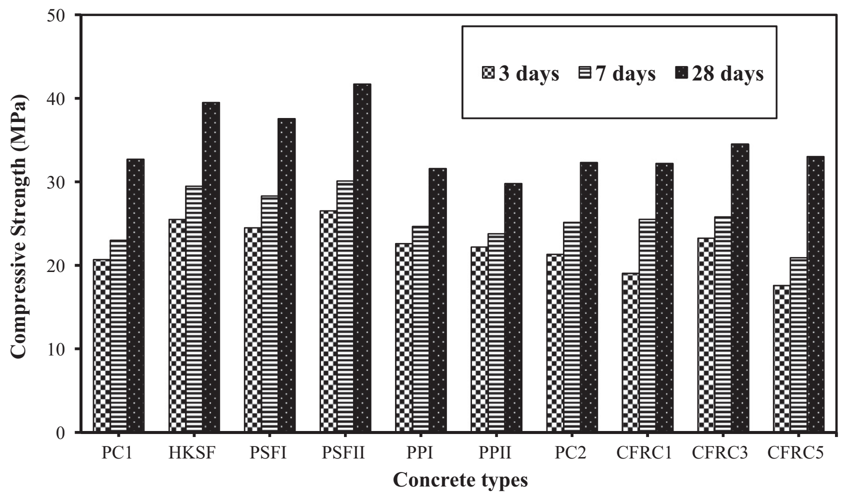

Fig. 4. Compressive strength of PC and various fibre reinforced concrete specimens at different ages.

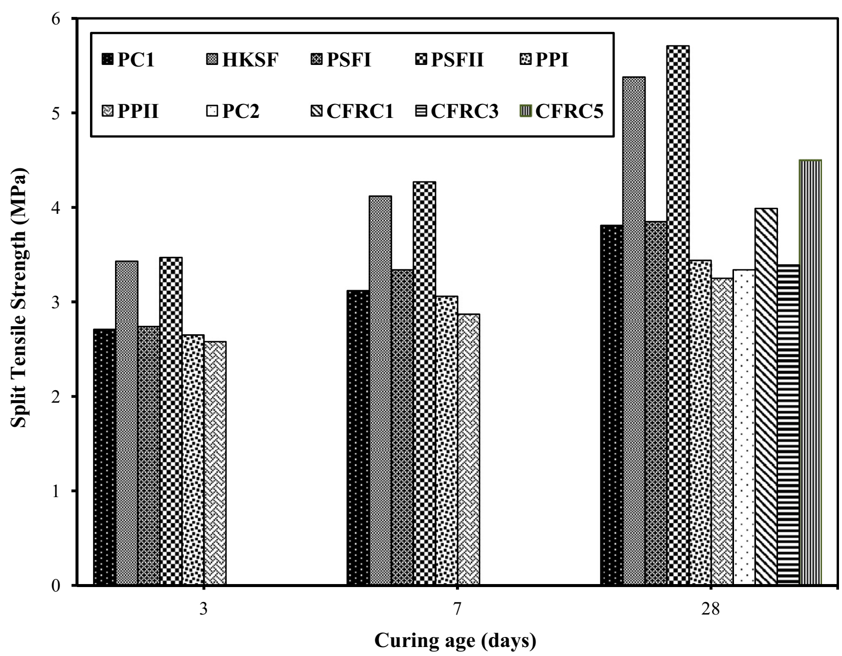

Fig. 5. Split tensile strength of PC and various fibre reinforced concrete specimens at different ages.

and properties of the fibre. Xu et al. [33] also obtained the best results for spiral II reinforced concrete among various types and shapes of fibre-reinforced concrete. The ultimate stress also increased with higher pressure, which is similar to the findings of Xu et al. [31] and Tan et al. [15].

In Figs. 7b and 8b, it can be seen that the ultimate stress of the concrete is significantly influenced by the addition of coir fibre. The percentage increments of ultimate stress for CFRC1, CFRC3 and CFRC5 are 20.26%, 31.9% and 72.19% at 2 MPa, whereas they are 14.8%, 38.64% and 76.6% at 3 MPa, respectively, when compared to PC2. Therefore, the ultimate stress of CFRC increases with the increment of pressure and coir fibre content.

Figs. 9 and 10 show the comparison of optimum stress–strain curves between three different fibre-reinforced concretes (CFRC5, PSFII and PPII) at 2 and 3 MPa pressure. Based on the figures, it is clear that CFRC5 shows much greater stress than PSFII and PPII. Therefore, it can be said that the dynamic ultimate stress of concrete significantly improves with the addition of 5% coir.

4.2.2. Ultimate strain

The ultimate strain and the strain rate of the PSFII reinforced specimen are higher than those for all the steel-type and polypropylene fibre-reinforced concrete specimens at the 2 and 3 MPa impact pressures, as shown in Figs. 7c and 8c. This is particularly clear under the 2 MPa impact load because the specimen with PSFII affects the specimen deformation rate under the same dynamic loading. This is followed by PSFI at 2 MPa and HKSF at 3 MPa. However, it can be seen that the ultimate strain of PPI is greater at 2 MPa but lower at 3 MPa. It can also be seen that the ultimate strain of different FRC specimens is affected by the shapes and properties of the fibres. The percentage increase in dynamic strains of the PSFII reinforced specimen are 25.2% and 21.98% at 2 and 3 MPa pressure, respectively, as compared to PC1.

Figs. 7c and 8c also show the strain rate values of PC2 and CFRC under the 2 MPa and 3 MPa loading pressures. When the loading pressure increases, the velocity of the applied impact force also increases and the strain rate typically improves. The strain rate

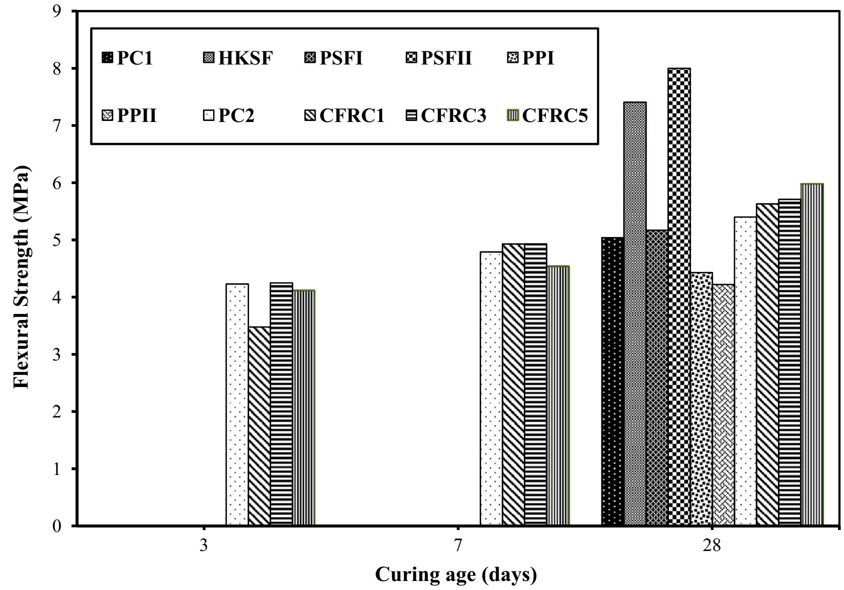

Fig. 6. Flexural strength of PC and various fibre reinforced concrete specimens at different ages.

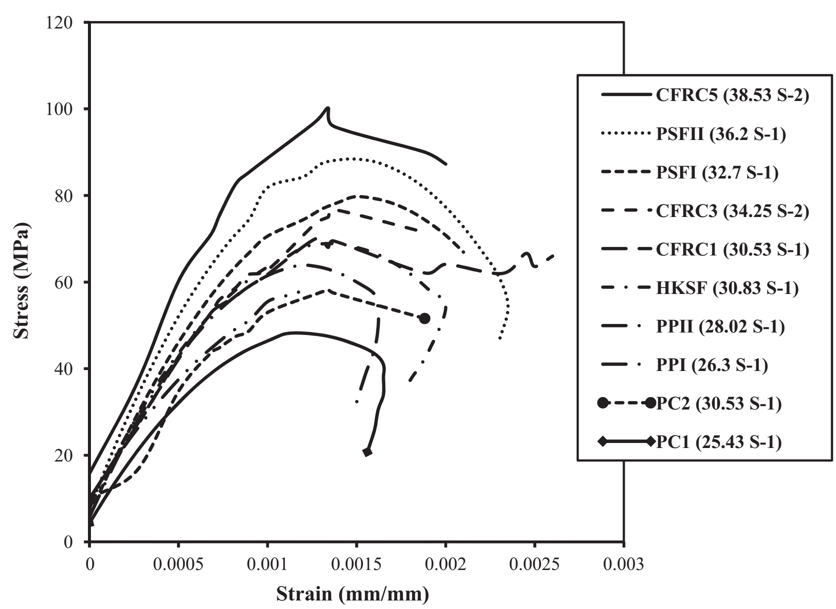

Fig. 7a. Stress–strain curves for concrete specimens of with and without reinforcement at 2 MPa pressure.

of CFRC is also influenced by the addition of coir fibre. Figs. 7c and 8c indicate that a higher coir fibre content results in a higher strain rate under both loading pressures. It can also be seen that the ultimate strain increases as the coir fibre content increases; thus, the ductility of the concrete increases with higher coir fibre content. This relationship between the coir fibre content and the ultimate strain is obvious for the specimens tested under a pressure of 3 MPa. However, specimens tested under a pressure of 2 MPa show a significant increase in ultimate strain (13.07%) for CFRC3 and a slight improvement (1.74%) for CFRC5 when compared to PC2. CFRC5 shows the maximum increase in ultimate strain, at approximately 126.3%, at 3 MPa pressure.

Therefore, it can be said that both the strain rate and the ultimate strain of the concrete significantly improved with the addition of 5% coir when considered for three different types of fibre (steel, polypropylene and coir).

4.2.3. Toughness

In this study, toughness is defined as the total area under the stress–strain curve up to the point of fracture. It is used to characterize the energy absorption capacity of the specimens [33]. The toughness property of PC and all types of reinforced concrete under 2 MPa and 3 MPa pressure is computed from Figs. 7a and 8a. Figs. 11a and 11b show the dynamic toughness of all types of FRC under 2 MPa and 3 MPa pressures. Table 5 shows the percentage increase in dynamic toughness of all types of FRC under 2 MPa and 3 MPa pressures. As shown in Figs. 11a and 11b and Table 5, the PSFII fibre-reinforced concrete has the highest toughness increment among all the tested specimens, which indicates the highest energy absorption capacity under similar impact pressure. The energy absorption capacity of the PSFII reinforced specimens are 162.2% and 146.4% higher than PC1 under 2 MPa and 3 MPa pressures, respectively. It is also observed that the toughness

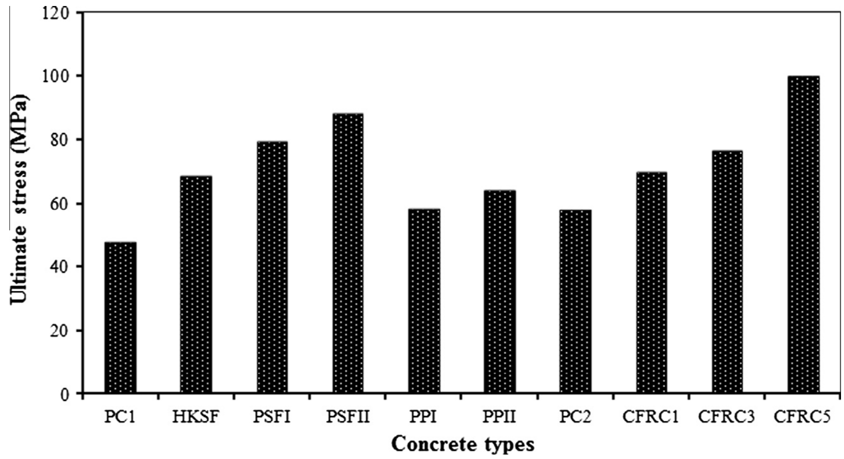

Fig. 7b. Ultimate stress for concrete specimens of with and without reinforcement at 2 MPa pressure.

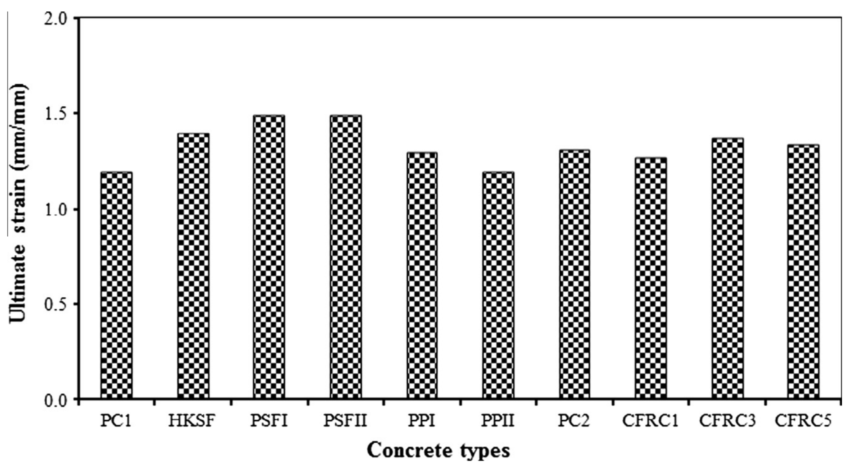

Fig. 7c. Ultimate strain for concrete specimens of with and without reinforcement at 2 MPa pressure.

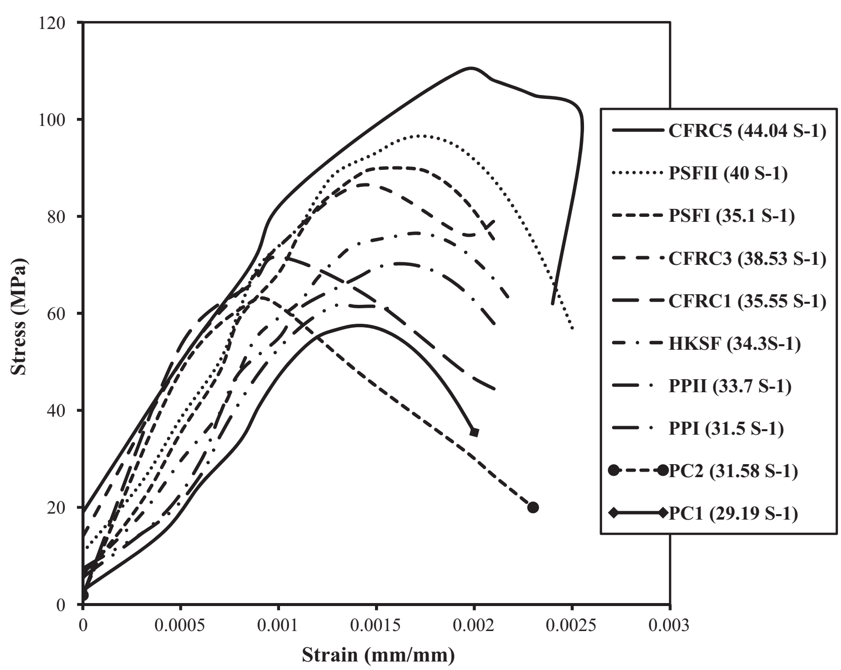

Fig. 8a. Stress–strain curves for concrete specimens of with and without reinforcement at 3 MPa pressure.

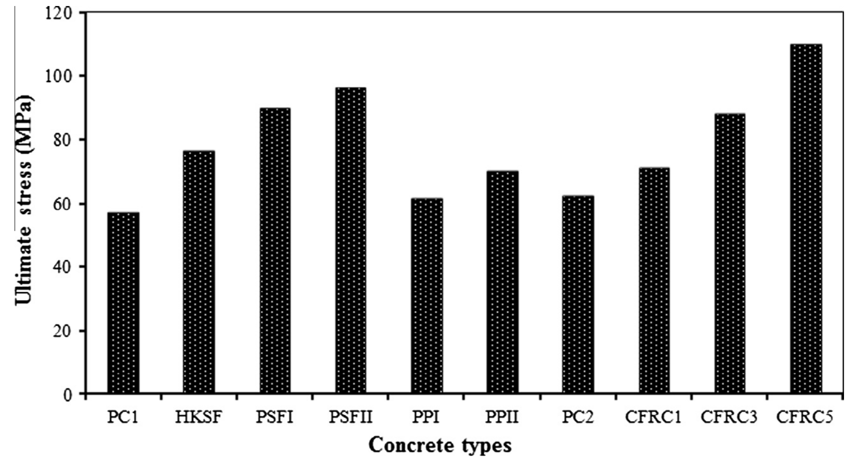

Fig. 8b. Ultimate stress for concrete specimens of with and without reinforcement at 3 MPa pressure.

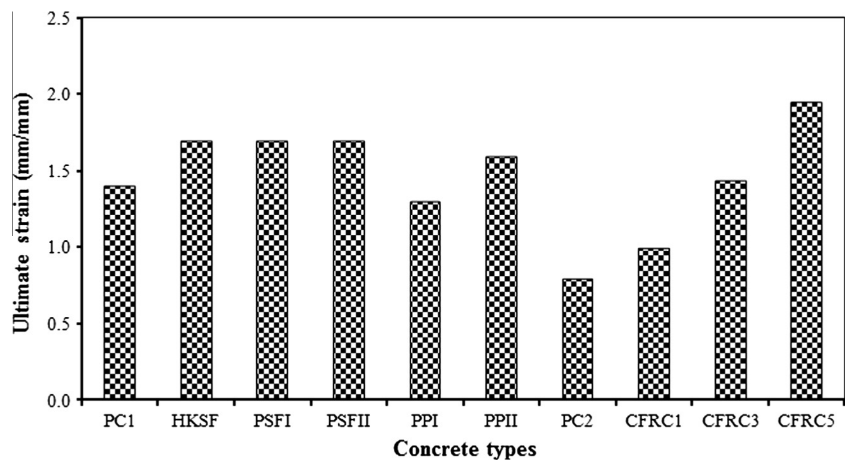

Fig. 8c. Ultimate strain for concrete specimens of with and without reinforcement at 3 MPa pressure.

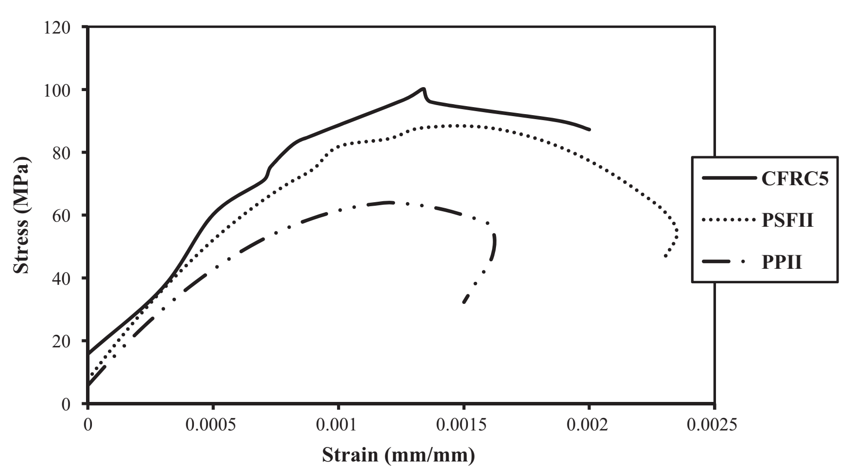

Fig. 9. Comparison in optimum stress–strain curves among three different fibre reinforced concrete at 2 MPa pressure.

increment of the PPI, PPII and HKSF specimens increase with impact pressure, while the toughness increment of the PSFI and PSFII specimens decrease with impact pressure compared to PC1. In addition, the strain rate of all the tested specimens increase with increasing impact velocity, which indicates that the energy absorption capacity is rate sensitive for the PC and FRC specimens. The energy absorption capacities and rate sensitivities are affected by the shapes and properties of the fibres. In addition, the toughness increases with the increment of pressure, which is similar to the findings of Xu et al. [33] and Tan et al. [17].

It can also be seen that the dynamic toughness of CFRC is significantly influenced by the addition of coir fibres. According to Table 5, the dynamic toughness of CFRC improves as the coir fibre content increases. The dynamic toughness indicates the ability of concrete

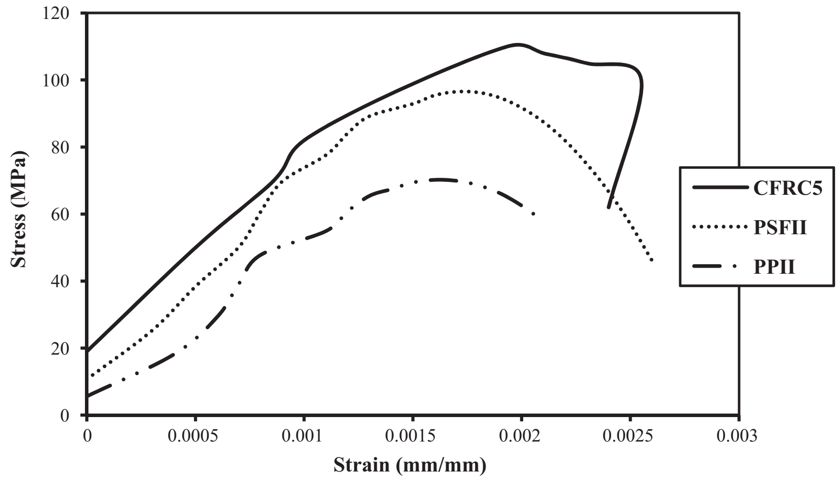

Fig. 10. Comparison in optimum stress–strain curves among three different fibre reinforced concrete at 3 MPa pressure.

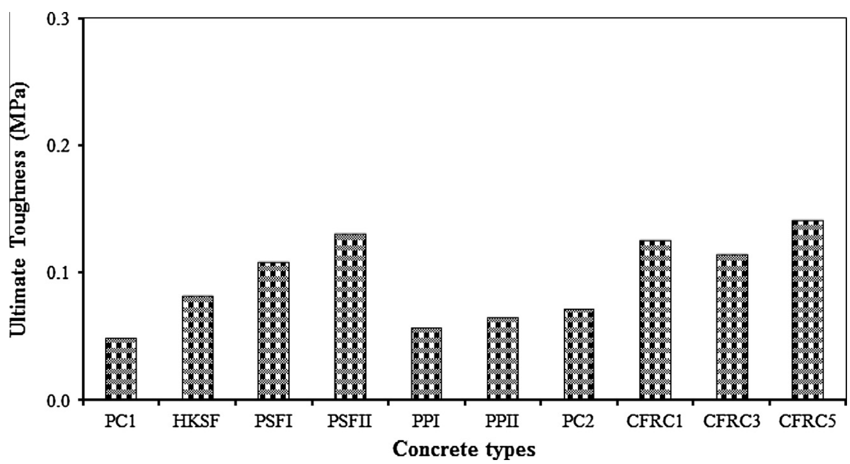

Fig. 11a. The toughness of different fibre reinforced concrete at 2 MPa pressure.

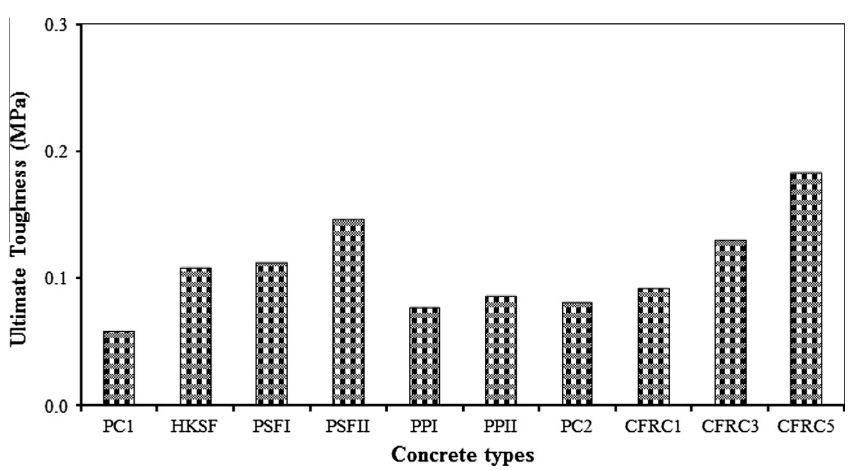

Fig. 11b. The toughness of different fibre reinforced concrete at 3 MPa pressure.

to absorb energy and plasticity deformation without fracturing. As a result, the energy absorption ability of CFRC significantly increases when the coir fibre content increases. The maximum increment in dynamic toughness of CFRC is 124.4% as compared to PC2.

Therefore, the increase in dynamic toughness is more significant in the PSFII reinforced concrete. However, the increase in dynamic toughness of CFRC5 is also comparable to the increase in dynamic toughness of the PSFII reinforced concrete.

Table 5
Overall static and dynamic performance of different fibre reinforced concretes.

Specimens.	Increase in Compressive strength (%)	Increase in Flexural strength (%)	Increase in Split tensile strength (%)	Increase in Dynamic Stress (%)		Increase in Dynamic Strain (%)		Increase in Dynamic Toughness (%)	
				At 2 MPa Pressure	At 3 MPa Pressure	At 2 MPa Pressure	At 3 MPa Pressure	At 2 MPa Pressure	At 3 MPa Pressure
HKSF	20.76	47	41.2	42.7	33.17	15.4	19.1	65.2	81.5
PSFI	14.86	2.6	1.1	65.3	56.15	21.9	6.4	117.4	88.9
PSFII	27.48	58.7	49.9	83.3	67.82	25.2	21.98	162.2	146.3
PPI	−3.4	−12.1	−9.7	21.26	6.92	9.8	8.51	15.2	29.6
PPII	−8.9	−16.3	−14.7	32.75	22.08	−2.44	14.9	30.4	44.4
CFRC1	−0.34	4.22	19.5	20.26	14.8	−4.26	19.07	72.6	13.4
CFRC3	6.9	5.63	1.5	31.9	38.64	13.07	69.3	57.5	59.8
CFRC5	2.23	10.73	34.7	72.19	76.6	1.74	126.3	94.5	124.4

5. Summary and conclusions

5.1. Static properties

(a) **Compressive strength**

The PSFII reinforced concrete displays the maximum increment in compressive strength at 27.48% at 3, 7 and 28 days, and the PP fibre-reinforced concretes (PPI & PPII) show a decrement in compressive strength at a later stage (28 days) of up to 3.4% and 8.9% as compared to PC1. In addition, the PSFI reinforced concrete shows a lower increment in compressive strength than commercial HKSF at all stages due to the risk of balling during mixing. According to the study by Holschemacher et al. [49], continuous corrugated steel reinforced concrete showed maximum compressive strength than hooked ends straight steel reinforced concrete. However, CFRC3 shows a 7% maximum improvement in compressive strength as compared to PC2.

(b) **Split tensile strength**

PSFII shows the maximum increment in split tensile strength at up to 30% at all ages, though significant at a later age (49.9%). However, the PSFI reinforced concrete shows a very small increment at all ages as compared with PC1. Holschemacher et al. [49] found significant improvement in split tensile strength of hook-end SFRC. The PP fibre-reinforced concretes (PPI & PPII) show decrements at all stages. However, CFRC5 shows a 35% maximum increment in split tensile strength when compared to PC2.

(c) **Flexural strength**

The PSFII reinforced concrete shows the most effective improvement in flexural strength at almost 50%, closely followed by the HKSF reinforced concrete (47%). Venkatesan et al. [50] reported the maximum increase of 41.34% deflection ductility for hook-ended SFRC beams with 1% volume fraction. The PP (PPI & PPII) fibre-reinforced concretes show 12% and 16% lower strength than PC1 at 28 days. However, CFRC5 shows an 11% improvement in flexural strength compared to PC2.

5.2. Dynamic properties

(a) **Ultimate stress**

Both the PSFI and PSFII reinforced concretes show greater ultimate stress (65.3% & 56.15%; 83.3% & 67.82%) compared to PC1 under both 2 MPa and 3 MPa impact pressures. Commercial HKSF reinforced concrete shows a lower increment of stress (42.7% & 33.17%) than PSFII and PSFI reinforced concretes under the same impact pressure. PP (PPI & PPII) reinforced concrete also shows an increment in ultimate stress over PC1, particularly in the PPII fibre-reinforced concrete (32.75% & 22.08%). However, CFRC5 exhibited a 95% and 124% maximum improvement in dynamic ultimate stress under 2 and 3 MPa pressures, respectively. Ali et al. [51] reported better dynamic response for mortar-free interlocking structures consisting of interlocking blocks where interlocking blocks were prepared with coconut fibre reinforced concrete.

(b) **Ultimate strain**

The increment of ultimate strain of the PSFII reinforced concrete is the highest (25.2% & 21.98%) among all the FRC specimens compared to PC1 under both 2 MPa and 3 MPa pressures. The ultimate stain increases proportionally with the impact pressure for all FRCs. The maximum 13% improvement of the dynamic ultimate strain under 2 MPa was recorded in CFRC3. However, CFRC5 exhibited a 126% maximum improvement of dynamic ultimate strain under 3 MPa pressure.

(c) **Toughness**

In this study, the PSFII fibre reinforced concrete shows a greater increment in toughness (energy absorption) properties (162.2% & 146.3%) than the other specimens under both 2 MPa and 3 MPa impact pressures. The dynamic toughness increases with the increment of impact pressure for the PPI, PPII and HKSF reinforced specimens; however, the PSFI and PSFII reinforced specimens show the reverse. In the CFRC specimens, the dynamic toughness improved as the coir fibre content increased. CFRC5 exhibited 94.5% and 124.4% maximum increments in dynamic toughness compared to PC2. Munawar et al. [52] reported that coir fibre is the toughest fibre (21.5 MPa) amongst all natural fibres, where toughness of a fibre is taken as the area under stress–strain curve.

Based on the overall experimental test results, the following conclusions are drawn from the present study

- The newly developed PSFII (W-shape steel fibre) reinforced concrete showed the significant improvement in static and dynamic properties.
- CFRC with 5% fibre exhibited more increment in dynamic comprehensive properties compared to static properties.
- FRC (reinforced with PP) showed negative/less influence on static properties, however the fibre improved the dynamic properties significantly.

Therefore, it can be concluded from the above results that the PSFII reinforced concrete shows the best static and dynamic properties due to its good bond between the concrete and the fibres. Moreover, CFRC5 also provides significant static and dynamic properties. Coir fibre stands at par with steel fibre in enhancing both the static and dynamic properties of FRC.

6. Recommendations

Steel fibre improved both the static and dynamic properties of concrete comprehensively. Therefore, it can be used to improve the structural strength to reduce the heavy steel reinforcement requirement. PP fibre has negative influence on the static properties of the concrete; however it shows significant influence on the dynamic properties. PPFRC can be recommended in preparation of structures under impact/moving loads, e.g. concrete pavement and bridge deck. CFRC has potential for sustainable concrete structure applications, e.g. roofing materials, wall panels/boards and columns. Using local materials such as coir fibres and ropes as reinforcement of concrete is more economical than the construction of earthquake-resistant structures with steel reinforcement.

Acknowledgements

The authors would like to acknowledge the financial support from Universiti Kebangsaan Malaysia through grants DLP-2013-033 and DIP-2014-019.

References

[1] S. Mindess, L. Zhang, Impact resistance of fibre-reinforced concrete, Proc. ICE-Struct. Build. 162 (1) (2009) 69–76.
[2] S. Vajje, N.R.K. Murthy, Study on addition of the natural fibers into concrete, Int. J. Sci. Technol. Res. 2 (11) (2013) 213–218.
[3] M. Sivaraja, Kandasamy, N. Velmani, M.S. Pillai, Study on durability of natural fibre concrete composites using mechanical strength and microstructural properties, Bull. Mater. Sci. 33 (6) (2010) 719–729.
[4] G. Ramakrishna, T. Sundararajan, Studies on the durability of natural fibres and the effect of corroded fibres on the strength of mortar, Cem. Concr. Compos. 27 (5) (2005) 575–582.
[5] V. Agopyan, H. Savastano Jr, V.M. John, M.A. Cincotto, Developments on vegetable fibre-cement based materials in São Paulo, Brazil: an overview, Cem. Concr. Compos. 27 (5) (2005) 527–536.
[6] P. Paramasivam, G.K. Nathan, N.C. Das Gupta, Coconut fibre reinforced corrugated slabs, Int. J. Cem. Compos. Light Concr. 6 (1) (1984) 19–27.
[7] Z. Li, L. Wang, X. Wang, Flexural characteristics of coir fiber reinforced cementitious composites, Fibers Polym. 7 (3) (2006) 286–294.
[8] M. Nili, V. Afroughsabet, Combined effect of silica fume and steel fibers on the impact resistance and mechanical properties of concrete, Int. J. Imp. Eng. 37 (2010) 879–886.
[9] M. Ali, A. Liu, H. Sou, N. Chouw, Mechanical and dynamic properties of coconut fibre reinforced concrete, Constr. Build. Mater. 30 (2012) 814–825.
[10] P.P. Yalley, A.S.K. Kwan, Use of coconut fibre as an enhancement of concrete, J. Eng. Technol. 2 (2012) 54–69.
[11] G.A.P. Gampathi, Application of coconut fibre in cement block industry, OIDA Int. J. Sust. Dev. 2 (9) (2011) 83–88.
[12] D.J. Cook, R.P. Pama, H.L.S.D. Weerasingle, Coir fibre reinforced cement as a low cost roofing material, Build. Environ. 13 (3) (1978) 193–198.
[13] W. Wang, N. Chouw, An experimental study of coconut fibre reinforced concrete under impact load, in: NZSEE Conference 2014 (Paper Number P34), Department of Civil and Environmental Engineering, University of Auckland, Auckland, New Zealand.
[14] N. Ganesan, T. Sekar, Permeability of steel fibre reinforced high performance concrete composites, J. Inst. Eng. (India) 86 (2005) 8–11.
[15] ACI Committee 544. State-of-the-Art Report on Fiber Reinforced Concrete ACI544.1R-96, Reapproved in 2002, ACI Committee 544 Report, ACI: Farmington Hills, MI, USA, 2002.
[16] E. Erdogmus, Use of fiber-reinforced cements in masonry construction and structural rehabilitation, Fibers 3 (2015) 41–63.
[17] C.Y. Tan, R. Hamid, M. Kasmuri, Dynamic stress–strain behaviour of steel fiber reinforced high-performance concrete with fly ash, Adv. Civil Eng. (2012) 1–6. Article ID 907431.
[18] P.K. Nagarkar, S.K. Tambe, D.G. Pazare, Study of fibre reinforced concrete, in: Proceeding of International Symposium of Fibre Reinforced Concrete, Madras, India, December 16–19, 1987, pp. 2131–2141.
[19] A.A.E. Aliabdo, A.E.M.A. Elmoaty, M. Hamdy, Effect of internal short fibers, steel reinforcement, and surface layer on impact and penetration resistance of concrete, Alex. Eng. J. 52 (2013) 407–417.
[20] Y. Hao, H. Hao, Dynamic compressive behaviour of spiral steel fibre reinforced concrete in split Hopkinson pressure bar tests, Constr. Build. Mater. 48 (2013) 521–532.
[21] J.G. Jang, H.K. Kim, T.S. Kim, B.J. Min, H.K. Lee, Improved flexural fatigue resistance of PVA fiber-reinforced concrete subjected to freezing and thawing cycles, Constr. Build. Mater. 59 (2014) 129–135.
[22] P. Suraneni, P.C.B. Anleu, R.J. Flatt, Factors affecting the strength of structural lightweight aggregate concrete with and without fibers in the 1200–1600 kg/m^3 density range, Mater. Struct., 2015 (corrected proof available in online).
[23] I.B. Topcu, M. Canbaz, Effect of different fibers on the mechanical properties of concrete containing fly ash, Constr. Build. Mater. 21 (7) (2007) 1486–1491.
[24] H. Wong, H.A. Razak, Efficiency of calcined kaolin and silica fume as cement replacement material for strength performance, Cem. Concr. Res. 35 (4) (2005) 696–702.
[25] C.S. Poon, S.C. Kou, L. Lam, Compressive strength, chloride diffusivity and pore structure of high performance metakaolin and silica fume concrete, Constr. Build. Mater. 20 (10) (2006) 858–865.
[26] O. Eren, T. Celik, Effect of silica fume and steel fibers on some properties of high-strength concrete, Constr. Build. Mater. 11 (7) (1997) 373–382.
[27] F. Koksal, F. Altun, I. Yigit, Y. Sahin, Combined effect of silica fume and steel fiber on the mechanical properties of high strength concretes, Constr. Build. Mater. 22 (8) (2008) 1874–1880.
[28] N. Banthia, S. Mindess, Impact resistance of steel fiber reinforced concrete, ACI Mater. J. 93 (5) (1996) 472–479.
[29] T.S. Lok, P.J. Zhao, G. Lu, Using the split Hopkinson pressure bar to investigate the dynamic behaviour of SFRC, Mag. Concr. Res. 55 (2) (2003) 183–191.
[30] Y. Lu, Q. Li, Appraisal of pulse-shaping technique in split Hopkinson pressure bar tests for brittle materials, Int. J. Prot. Struct. 1 (3) (2010) 363–390.
[31] Z.L. Wang, Z.M. Shi, J.G. Wang, On the strength and toughness properties of SFRC under static-dynamic compression, Compos. Part B Eng. 42 (2011) 1285–1290.
[32] R. Hamid, K.R. Jamalluddin, A.S.M.Z. Hasan, Dynamic stress and strain of HPC under drop-weight impact loading, J. Tek. 65 (2) (2013) 29–35.
[33] Z. Xu, H. Hao, H. Li, Experimental study of dynamic compressive properties of fibre reinforced concrete material with different fibres, Mater. Des. 33 (2012) 42–55.
[34] N. Banthia, C. Yan, K. Sakai, Impact resistance of fiber reinforced concrete at subnorma temperatures, Cem. Concr. Compos. 20 (5) (1998) 393–404.
[35] A.E. Naaman, Tridimensional Fiber Reinforcement of Portland Cement Concrete Matrices, US3852930 A, 1974.
[36] A.E. Naaman, Fiber reinforcement for concrete, Concr. Int. 7 (1985) 21–25.
[37] J. Alwan, A.E. Naaman, P.A. Guerrero, Effect of mechanical clamping on the pull-outresponse of hooked steel fibers embedded incementitious matrices, Concr. Sci. Eng. 1 (1) (1999) 15–25.
[38] A.E. Naaman, H.W. Reinhardt (Eds.), High Performance Fiber Reinforced Cement Composites: HPFRCC 2. RILEM, No. 31, London, E. & FN Spon, 1996.
[39] A.E. Naaman, Engineered steel fibers with optimal properties for reinforcement of cement composites, J. Adv. Concr. Technol. 1 (3) (2003) 241–252.
[40] ASTM C150, Standard specification for Portland cement, ASTM C150-07, Annual Book of ASTM Standard, vol. 04.01, 2009, pp. 152–157.
[41] BS EN 12390-3, Testing hardened concrete, Compressive strength of test specimens, BSI, London, 2002.
[42] ASTM C496/C496M-04, Standard test method for splitting tensile strength of cylindrical concrete specimens, Annual Book of ASTM Standard, West Conshohocken, PA, 2004.
[43] BS 1881-117:1983 – Testing concrete, Method for Determination of Tensile Splitting Strength, Milton Keynes, UK, 2009.
[44] BS 1881-118:1983 – Testing concrete, Method for Determination of Flexural Strength, Milton Keynes, UK, 2009.
[45] P. Song, S. Hwang, Mechanical properties of high-strength steel fiber-reinforced concrete, Constr. Build. Mater. 18 (9) (2004) 669–673.
[46] Y. Mohammadi, S. Singh, S. Kaushik, Properties of steel fibrous concrete containing mixed fibres in fresh and hardened state, Constr. Build. Mater. 22 (5) (2008) 956–965.
[47] B.P. Hughes, N.I. Fattuhi, Load–deflection curves for fibre-reinforced concrete beams in flexure, Mag. Concr. Res. 29 (101) (1977) 199–206.
[48] A.M. Neville, Properties of Concrete, fourth ed., Pearson Education Ltd., Essex, England, 2005.
[49] K. Holschemacher, T. Mueller, Y. Ribakov, Effect of steel fibers on mechanical properties of high strength concrete, Mater. Des. 31 (2010) 2604–2615.
[50] K.R. Venkatesan, P.N. Raghunath, K. Suguna, Flexural behavior of high strength steel fibre reinforced concrete beams, Int. J. Eng. Sci. Inn. Tech. 4 (1) (2015) 135–140.
[51] M. Ali, R. Briet, N. Chouw, Dynamic response of mortar-free interlocking structures, Constr. Build. Mater. 42 (2013) 168–189.
[52] S.S. Munawar, K. Umemura, S. Kawai, Characterization of the morphological, physical, and mechanical properties of seven non-wood plant fibre bundles, J. Wood Sci. 53 (2) (2007) 108–113.